HHS Public Access

Author manuscript

Histochem Cell Biol. Author manuscript; available in PMC 2016 April 04.

Published in final edited form as:

Histochem Cell Biol. 2009 December ; 132(6): 585–597. doi:10.1007/s00418-009-0639-4.

Altered expression of $P2X_3$ in vagal and spinal afferents following esophagitis in rats

Banani Banerjee,
Division of Gastroenterology and Hepatology, Medical College of Wisconsin, 8701 Watertown Plank Road, Milwaukee, WI 53226, USA

Bidyut K. Medda,
Division of Gastroenterology and Hepatology, Medical College of Wisconsin, 8701 Watertown Plank Road, Milwaukee, WI 53226, USA

Jamie Schmidt,
Division of Gastroenterology and Hepatology, Medical College of Wisconsin, 8701 Watertown Plank Road, Milwaukee, WI 53226, USA

Yue Zheng, **Zhihong Zhang**,
Division of Gastroenterology and Hepatology, Medical College of Wisconsin, 8701 Watertown Plank Road, Milwaukee, WI 53226, USA

Reza Shaker, and
Division of Gastroenterology and Hepatology, Medical College of Wisconsin, 8701 Watertown Plank Road, Milwaukee, WI 53226, USA

Jyoti N. Sengupta
Division of Gastroenterology and Hepatology, Medical College of Wisconsin, 8701 Watertown Plank Road, Milwaukee, WI 53226, USA

Banani Banerjee: banerjee@mcw.edu

Abstract

Purinergic $P2X_3$ receptors are predominantly expressed in small diameter primary afferent neurons and activation of these receptors by adenosine triphosphate is reported to play an important role in nociceptive signaling. The objective of this study was to investigate the expression of $P2X_3$ receptors in spinal and vagal sensory neurons and esophageal tissues following esophagitis in rats. Two groups of rats were used including 7 days fundus-ligated (7D-ligated) esophagitis and sham-operated controls. Esophagitis was produced by ligating the fundus and partial obstruction of pylorus that initiated reflux of gastric contents. The sham-operated rats underwent midline incision without surgical manipulation of the stomach. Expressions of $P2X_3$ receptors in thoracic dorsal root ganglia (DRGs), nodose ganglia (NGs), and esophageal tissues were evaluated by RT–PCR, western blot and immunohistochemistry. Esophageal neurons were identified by retrograde transport of Fast Blue from the esophagus. There were no significant differences in $P2X_3$ mRNA

Correspondence to: Banani Banerjee, banerjee@mcw.edu.

Present Address: Y. Zheng, Department of Gastroenterology, First Hospital Peiking University, No. 8 Xi Shiku Street, 100034 Beijing, People's Republic of China

expressions in DRGs (T1–T3) and NGs between 7D-ligated and sham-operated rats. However, there was an upregulation of $P2X_3$ mRNA in DRGs (T6–T12) and in the esophageal muscle. At protein level, $P2X_3$ exhibited significant upregulation both in DRGs and in NGs of rats having chronic esophagitis. Immunohistochemical analysis exhibited a significant increase in $P2X_3$ and TRPV1 co-expression in DRGs and NGs in 7D-ligated rats compared to sham-operated rats. The present findings suggest that chronic esophagitis results in upregulation of $P2X_3$ and its co-localization with TRPV1 receptor in vagal and spinal afferents. Changes in $P2X_3$ expression in vagal and spinal sensory neurons may contribute to esophageal hypersensitivity following acid reflux-induced esophagitis.

Keywords

$P2X_3$ receptor; Dorsal root ganglia; Vagus; Acid reflux; Esophagitis

Introduction

The excitability of primary sensory neuron innervating the gastrointestinal (GI) tract is enhanced following injury, ischemia, and visceral inflammation (Cooke et al. 2003; Holzer 2001; Kirkup et al. 2001). In recent years, purinergic neurotransmitter adenosine tri-phosphate (ATP) has been widely recognized as a fast synaptic neurotransmitter in both peripheral and central neurons and activation of various purinergic receptors is reported to play an important role in nociceptive signaling (Bardoni et al. 1997; Evans 1996; Khakh et al. 1995; Sawynok and Reid 1997). Growing evidence supports the involvement of purinergic P2X receptors in nociception where ATP released from epithelial cell lining of the gastrointestinal (GI) tract, bladder, and ureter activates P2X receptors present on subepithelial nerve plexus and the signal is transmitted via the spinal cord to the brain (Burnstock 2006). This hypothesis has been supported in recent study documenting that the $P2X_3$ knockout mice exhibits reduction of micturition reflex and attenuation of pain behavior (Cockayne et al. 2000). It has also been shown that the $P2X_3$ expression in DRG neurons can be altered by chronic nerve injury, axotomy, and in neuropathic pain (Bradbury et al. 1998; Novakovic et al. 1999).

Immunohistochemical studies in rats have demonstrated that $P2X_3$ receptors are mainly expressed in IB4-positive small diameter cells in DRGs (Vulchanova et al. 1998). The central projections of these neurons are in the inner lamina II of the spinal dorsal horn and the peripheral terminals innervate the skin, corneal epithelium, and sub-epithelial regions of hollow viscera (Guo et al. 1999; Robinson et al. 2004; Vulchanova et al. 1998; Xiang and Burnstock 2004). $P2X_3$ receptors are expressed predominantly in DRGs, whereas cells of nodose ganglia (NGs) have mixed population of $P2X_2$ and heteromeric $P2X_{2/3}$ receptors (Bradbury et al. 1998; Dunn et al. 2001, Novakovic et al. 1999; Vulchanova et al. 1997; Xiang et al. 1998). In NGs, $P2X_2$ and $P2X_3$ are mostly identified in the same neurons and similar co-localization is found in the nucleus tractus solitarius (Vulchanova et al. 1997; Xiang et al. 1998). In contrast, there is hardly any co-localization in the dorsal horn neurons (Vulchanova et al. 1997). These differences in P2X receptors expression patterns are also

consistent with the differences in the pharmacological properties of P2X receptors expressed in NG and DRG neurons (Dunn et al. 2001).

It has been documented that visceral afferent fibers undergo sensitization following visceral inflammation. For example, vagal mechanosensitive afferents innervating the esophagus of ferrets exhibit significantly greater response to $P2X_3$ receptor agonist α,β-methylene ATP following esophagitis (Page et al. 2000). Although immunohistochemistry and molecular biology data indicate that $P2X_3$ is the predominant purinergic receptor subunit expressed by sensory neurons, no systematic study has been carried out on $P2X_3$ expression and upregulation in DRGs and NGs in esophageal hypersensitivity. Therefore, the present study was undertaken to address the influence of reflux-induced esophageal injury on the overall expression profile of $P2X_3$ receptors in thoracic spinal and vagal sensory neurons and its expression in esophageal tissues. The differential expression pattern of $P2X_3$ receptors in vagal and spinal sensory neurons innervating the esophagus and its alteration following inflammation may indicate the relative contribution of these two pathways in esophageal hypersensitivity.

Method

Surgical procedure for promoting reflux

Adult male Sprague–Dawley rats were used according to the protocol approved by Institutional Animal Use and Care Committee of Medical College of Wisconsin. According to the protocol, rats weighing 200–250 g were fasted overnight and anesthetized by injecting a mixture of ketamine (100 mg/kg, i.p.) and xylazine (10 mg/kg, i.p). Two groups of rats were used in this study. The control group (sham-operated) rats were operated with only midline incision and digital manipulation of the stomach. In experimental group (7D-ligated), chronic reflux esophagitis was developed by following the methods as described earlier (Omura et al. 1999). In brief, the abdomen was opened by giving a 3- to 4-cm-long midline incision and latex ring (2 mm in thickness; ID, 5–6 mm; OD, 8–9 mm) made from 18-Fr Nalaton catheter was placed around the area of pyloric sphincter in order to restrict gastric emptying. The transitional region (i.e. limiting ridge) between the fundus and the glandular portion of the stomach was ligated with 2–0 silk thread to restrict the compliance of the stomach, which resulted in reflux of gastric contents into the esophagus. Rats were treated with antibiotic (Enrofloxacin, 2.5 mg/kg, im., SID) and analgesic (Rimadyl, 5 mg/kg, sc SID) to prevent infection and pain, respectively. All rats were euthanized 7 days after the surgery. The paraffin-embedded sections of distal esophagus from both the groups were subjected to Hematoxylin and Eosin (H&E) staining.

Surgical procedure for retrograde labeling

A week prior to reflux-promoting surgery (see previous section), rats were fasted overnight and anesthetized by injecting a mixture of ketamine (100 mg/kg, i.p.) and xylazine (10 mg/kg, i.p). The upper part of the abdomen below sternum was opened by a midline incision. The stomach was retracted to access the subdiaphragmatic esophagus and four injections each containing 2.0 μl of 4% Fast Blue solution (Polyscience, Warrington, PA) was applied into the muscle. Following injection, the needle was kept in place for at least 1

min to avoid the leakage of the dye. The injection site was carefully swabbed with saline before closing the wound to avoid non-specific labeling. The abdomen was closed in layers by suturing muscle followed by skin. Rats were treated with antibiotic and analgesic as described in the previous section. The dye-injected sites were directly examined under epifluorescent illumination, to determine the distribution of tracer near the injection site and also to examine any possible spreading near the injection site. For retrograde labeled neurons in DRGs and NGs, we noticed a very faint staining in most of the cells, which may be due to a slight vascular spread of the tracer from the injected site. However, the difference in labeling intensity between these cells and those labeled by axonal transport was very striking and did not cause any problem in identification of the actual retrogradely labeled cells.

Tissue extraction and storage

For quantitative PCR and western blot, rats were deeply anesthetized with sodium pentobarbital (60 mg/kg, ip) and thoracic laminectomy was performed to remove DRGs (T1–T3) and (T6–T12) bilaterally. The NGs from either side were approached ventrally below the cranial bone and were removed. Thorax was opened to access the esophagus and was transected just caudal to the upper esophageal sphincter (UES). A second transection was made on the cardia just below the lower esophageal sphincter (LES). A ligature was placed near the cardia and the thread was passed through the esophageal lumen to the proximal end. The mucosal layer was separated from the muscle layer at the proximal end under the microscope and was tied. The thread was then pulled distally with a steady motion to separate the mucosa from the muscle layer. All tissues were stored in liquid nitrogen at −80°C until used for further experiments. Following tissue extraction, rats were euthanized by injecting 0.25 ml/kg of Beuthanasia-D (390 mg pentobarbital + 50 mg phenytoin sodium + 2% benzyl alcohol; Schering-Plough, USA).

For immunohistochemistry, rats were deeply anesthetized with sodium pentobarbital (50 mg/kg, ip) and the chest was opened by mid-sternal incision. Animals were perfused transcardially with 300 ml of ice-cold phosphate buffer solution followed by 4% paraformaldehyde in 0.1 M PBS (pH 7.4). Bilateral thoracic DRGs and NGs were collected and incubated in 4% paraformaldehyde overnight at 4°C. Tissues were cleaned of connective tissues and cryoprotected in 20% sucrose in PBS for 24 h.

$P2X_3$ mRNA expression in thoracic DRGs (T1–T3 and T6–T12), NGs, and esophagus

Real-time RT–PCR was performed for accurate quantification of the target gene. The method was based on the measurement of PCR product during the amplification thermocycles by using SYBR Green fluorescent dye. A threshold for detection of the PCR product was set within the exponential interval of PCR amplification and was measured as C_T, the number of PCR cycles required to obtain this threshold. For acquiring enough tissue for cDNA preparation, DRGs and NGs from two rats were pooled together and similarly three preparations each for two sets of DRGs and NGs were made by using total of six animals per group. The primer sets for $P2X_3$ was designed using molecular Becon program (Premier BioSoft International, Palo Alto, CA). The PCR reactions were performed using iQ SYBR Green Supermix (BIO-RAD), 5 pmole forward and reverse primers, and 2 μl cDNA

from each tissue sample as template in a total of 25 μl of the reaction mixture. PCR reactions were carried out in 96-well microtiter plates and the samples were incubated for 3 min at 95°C and were amplified for 45 cycles of 10 s at 95°C and 30 s at 57°C. $P2X_3$ (sense) 5′ AGTCCTCAGTAGTTACAAAG 3′, $P2X_3$ (antisense) 5′ ACTTCTCTTCATTCTCTGG 3′, GAPDH (sense) 5′ CCTGCCAAGTATGATGAC 3′, GAPDH (antisense) 5′ GGAGTTGCTGTTGAAGTC 3′. To verify the amplification efficiency within each experiment, a serial dilution of cDNA derived from a RNA pool of control tissues was amplified in triplicate in each plate. The specificity of PCR reaction and possibility of primer dimerization were verified using melt curve program and no template control for each PCR reaction. As all PCR reactions were performed with equal efficiencies, the relative mRNA expression level of the target gene was directly normalized against the expression level of reference gene GAPDH for the same tissue sample. The C_T values for reference gene GAPDH were highly reproducible between samples and between PCR reactions. The cDNA preparations with C_T values <35 were considered as specific amplification and reactions with C_T values >35 were not included in the study. Results were expressed as relative mRNA expression in terms of C_T values in relation to the amount of reference gene mRNA expression using formula = $2^{-(CTtarget - CTGAPDH)}$.

Western blot analysis of $P2X_3$ protein in DRGs (T1–T3 and T6–T12), NGs, and esophagus

As mentioned for cDNA preparation, DRGs, and NGs from two rats were pooled together and similarly three preparations each from thoracic DRGs and NGs were made by using total of six animals per group. Crude extracts from various rat tissues were prepared by powdering the tissues in liquid nitrogen and homogenization in ice cold hypotonic lysis buffer (10 mM Tris–HCl, 5 mM EDTA, pH 8.0) containing protease inhibitor cocktail tablet (Complete Mini, Roche Diagnostics, Indianapolis, IN) and phosphatase inhibitor cocktail (Thermo Scientific, Rockford, IL), followed by differential centrifugation first at 1,200 rpm for 30 min and then for another 30 min at 14,000 rpm. The membrane pellet was solubilized for 30 min on ice with RIPA buffer (150 mn NaCl, 50 mM Tris–HCl, pH 7.5, 1 mM EDTA, 1 mM PMSF,1% Triton X-1000, 0.5% Na-deoxycholate, 0.1% sodium dodecyl sulphate (SDS) containing protease and phosphatase inhibitors). The membrane extracts were centrifuged and were assayed for protein content by BCA method (Thermo Fisher Scientific Inc., Rockford, IL, USA). Approximately, 25 μg of tissue extract from various samples was electrophoresed on 8% SDS PAGE and was transferred onto nitrocellulose membrane. After transfer, the membrane was blocked with 5% nonfat milk then probed with antibodies to $P2X_3$ (Rabbit anti $P2X_3$, 1:1000, Alomone Labs, Jerusalem, Israel). Protein bands were visualized using a horseradish peroxidase conjugated secondary antibody (Jackson Immununo-Research, West Grove, PA, USA) and an enhanced chemoluminiscent detection system (Thermo Scientific Inc.). To examine the specificity of $P2X_3$ antibody used in this study, the antibody was preabsorbed with the blocking peptide (1 μg peptide for 1 μg antibody) overnight at 4°C and used for immunoblotting. The relative changes in the intensity of $P2X_3$ protein expression in various samples were normalized against the intensity of house keeping gene β-actin for the same tissue sample using alpha imager 3400 software (Alpha Innotech, San Leandro, CA).

Immunohistochemical evaluation of $P2X_3$ expression in thoracic DRGs (T1–T3 and T8–10) and NGs

For immunostaining, tissues were embedded in histoprep (Fisher Scientific, Pittsburgh, PA, USA) and serial sections of 20 μm thickness were cut on a cryostat. Sections were rehydrated in PBS and non-specific sites were blocked by incubating the sections in PBS containing 10% normal goat serum (NGS), 0.5% Triton X-100 and 0.01% sodium azide for 60 min at room temperature. For double immunofluorescence staining with TRPV1 and $P2X_3$ antibodies, sections were incubated with a mixture of guinea pig anti-TRPV1 antibody (1:500; Chemicon International Inc. Temecula, CA, USA) and rabbit anti-$P2X_3$ antibody (1:500; Alomone) overnight at 4°C. The antibody dilution was carried out in PBS containing 3% NGS, 0.3% Triton X-100 and 0.01% azide (antibody diluent). Secondary antibodies used for double labeling were Alexa 488-conjugated goat anti-guinea pig antibody (1:500) and Alexa 568-conjugated goat anti-rabbit antibody (1:2000). For double immunostaining with $P2X_3$ and isolectin-B4 (IB4), tissue sections from DRGs and NGs were incubated with biotin-labeled IB4 at 10 μg/ml (Sigma, St. Louis, MO, USA) along with rabbit anti-$P2X_3$ antibody (1:1000; Alomone). Secondary antibodies used were Alexa-488-conjugated streptavidin peroxidase (1:1000) and Alexa 568 conjugated goat anti-rabbit antibody.

For double immunostaining with $P2X_3$ and Substance P (SP), primary antibodies used were guinea pig anti-SP (1:500,) and rabbit ant-$P2X_3$ (1:1000, Alomone). The secondary antibodies used were Alexa 488-conjugated goat anti-guinea pig (1:500) and Alexa 568-conjugated goat anti-rabbit (1:2000) antibodies. All the secondary antibodies used in this study were purchased from Molecular Probes (Invitrogen Corporation, Carlsbad, CA, USA). The specificity of the primary antibodies was assessed by pre-incubating the antibody overnight at 4°C with the immunizing peptides (10 μM) prior to the application to tissue sections. Tubes containing the same dilution of antibody, but without any addition of peptides were incubated in parallel. The absorbed and non-absorbed antibodies were incubated with the DRG and NG sections for 24 h at 4°C. Some sections in every run were incubated with either PBS instead of primary antibody or antibodies that were pre-absorbed with the corresponding peptide antigens. Slides were examined under a fluorescence microscope (Nikon Eclipse 50i) using narrow band cubes for Alexa 488 (DM505, excitation filter 470–490, barrier filter 515–550 nm) and Alexa 568 (DM 568, excitation filter 540–560, barrier filter 575–645 nm). Images were captured with a Spot II high-resolution digital camera (Diagnostic Instruments Inc., Sterling Heights, MI, USA) and were processed with Adobe Photoshop program. Each color of double-labeled DRG/NG sections were digitally imaged at 20× using filter sets for Alexa 488 (green) and Alexa 568 (red). Three sections each from sham-operated controls and experimental groups were used for counting the cells with positive staining and were calculated as mean ± SD.

Data analysis

For statistical analysis, thoracic T3, T8, and NG were selected. The entire DRGs, NGs were sectioned (20 μm) by taking one and skipping four sections and stained. Investigators were blinded to all treatments in all experiments. Three sections per tissue were selected for intensity measurement. The staining intensity of the selected cells was threshold, quantified, and averaged per tissue section using Metamorphic Imaging software (Molecular Devices,

Sunnyvale, CA, USA). The merged images were decoded and the intensity of staining was measured by selecting individual cells using region specific tools.

To maintain the consistency of image capturing, we used the same time exposure, gain and gamma adjustment for the control and the experimental samples for each fluorescence staining. We used the curve program of Adobe Photoshop (CS2) for the background adjustment to enable the counting of total number of cells. To define the cells with positive staining, we set up different cut off for mean intensity for the small and medium/large diameter cells based on the background using Image J program (Bethesda, MD, USA). A cell with soma containing a darker nucleus was only selected for cell count and similarly for the measurement of intensity of staining, ten random cells were selected for each DRG and NG section. For data analyses, cell counts and intensity measurement were carried out in sections from three animals in each group and were presented as mean ± SD. Statistical analyses between two groups were performed using paired *t* test. *P* value of less than 0.05 was considered significant.

Results

H&E staining of esophageal tissues

Macroscopical examination revealed tissue injuries (hemorrhage, erosion, and vascularization) in entire thoracic and abdominal (subdiaphragmatic) esophagus of 7D-ligated rats. Histological examination of H&E stained esophagus from 7D-ligated rats exhibited marked increase in thickness, edema of epithelial cell layers, basal cell, and lamina propria. In addition, an extensive submucosal hyperplasia along with numerous inflammatory cell infiltration within the submucosa was observed (Fig. 1b, d). In contrast, esophagus of sham-operated rat exhibited a thin epithelial layer with intact mucosa and very few inflammatory cells in the submucosal layers (Fig. 1a, c).

Quantitative estimation of $P2X_3$ mRNA expression in DRGs, NGs, and esophagus

The quantitative estimation of $P2X_3$ mRNA expression in DRGs, NGs, and distal esophagus from sham-operated and 7D-ligated rats was determined using real time PCR. Although it was not statistically significant (0.07 ± 0.02 vs. 0.034 ± 0.014 in sham, $P = 0.08$, $n = 3$), the mRNA expression in the DRGs (T1–T3) from 7D-ligated esophagitis rats exhibited two-fold increase compared to sham-operated rats (Fig. 2a), whereas, a significant increase in $P2X_3$ gene expression was observed in lower thoracic DRGs (T6–T12) from the ligated rats (0.05 ± 0.01 vs. 0.03 ± 0.01 for controls, $P < 0.05$, Fig. 2b). On the other hand, no significant difference was observed in $P2X_3$ expression in NGs between 7D-ligated and sham-operated rats (0.049 ± 0.017 vs. 0.038 ± 0 01 for controls, Fig. 2c). The esophageal tissue was separated into mucosal and muscle layers and the cDNA preparations were subjected to real time PCR (Fig. 3a, b). In the mucosa, no significant difference in $P2X_3$ mRNA expression was observed between the 7D-ligated esophagitis and sham-operated rats (0.026 ± 0.008 vs. 0.03 ± 0.017 in sham-operated rats, Fig. 3a). In contrast, a significant increase in mRNA expression (0.17 ± 0.05 vs. 0.08 ± 0.026 in sham-operated rats, $P < 0.05$) was observed in the muscle layers (Fig. 3b). Therefore, the analysis of $P2X_3$ mRNA expression in various tissues from sham-operated and 7D-ligated rats revealed diverse expression pattern.

$P2X_3$ protein expression profile in DRGs, NGs, and esophagus

Bilateral DRGs (T1–T3), (T6–T12), and NGs from sham-operated and 7D-ligated animals were analyzed by immunoblots for $P2X_3$ protein expression (Fig. 4a). In sham-operated rats, the anti-$P2X_3$ antibody exhibited immunoreactivity in the molecular range of 50 kDa for DRGs and NGs (Fig. 4a). The immunoreactive bands appeared as doublets (two very closely migrated bands in the molecular weight range of 50–55 kDa). To confirm the specificity of the reaction, we used primary antibody pre-absorbed with control peptides for immunoblot analysis of DRGs and NGs protein samples from sham-operated animals. The $P2X_3$ antibody pre-absorbed with immunogen completely blocked the immunoreactivity of the lower band from the doublets confirming the specificity of the reaction (Fig. 4b). The chronic esophagitis resulted in significant increase in $P2X_3$ protein expression both in DRGS (T1–T3) and (T6–T12) compared to sham-operated controls, $P < 0.01$ measured as relative intensity of expression against β-actin (Fig. 4c). Similarly, in the NGs, a significant increase in $P2X_3$ protein expression was observed in 7D-ligated group compared to controls, $P < 0.05$ (Fig. 4a, c).

In muscle and mucosa, a differential expression of $P2X_3$ protein was observed with predominantly higher expression in muscle compared to mucosal layers (Fig. 5a, b). Both in muscle and in mucosa, $P2X_3$ protein was expressed at 64 kDa. There was no significant difference in $P2X_3$ protein in both mucosa and muscle from 7D-ligated esophagitis rats compared to sham-operated rats.

Immunohistochemical analysis of $P2X_3$ staining in DRGs and NGs

Both in DRGs and NGs, $P2X_3$-immunoreactivity ($P2X_3$-ir) was mainly observed in small- and medium-sized neurons and the intensity of staining was relatively higher in cells from the 7D-ligated rats compared to sham-operated controls (Fig. 6). The $P2X_3$-positive cells in upper thoracic (T3) and lower thoracic (T8) DRGs from 7D-ligated were 33 ± 4.5 and 32 ± 3.0%, respectively. The percentage of $P2X_3$-positive cells in sham-operated controls were 32.5 ± 6.6% in T3 and 30 ± 5% in T8 DRGs, indicating no significant difference in $P2X_3$ receptor expression between the experimental and control groups. In NGs, $P2X_3$-positive cells from 7D-ligated and sham-operated rats were 71.63 ± 10.06 and 61.7 ± 6.2%, respectively. However, the mean intensity of $P2X_3$ staining as measured for individual DRG cells exhibited a significant increase in 7D-ligated group compared to sham-operated controls. The mean intensity of $P2X_3$ staining for T3 DRGs from 7D-ligated rats was 26.1 ± 2.99 compared to 14 ± 2.78 for sham-operated controls ($P < 0.01$). Similarly, the mean intensity of staining for T8 DRGs from 7D-ligated rats was 30 ± 3.5 versus 20 ± 4.8 for sham-operated group ($P < 0.01$). For NGs, a significant increase in the intensity of $P2X_3$ staining for individual cells was also observed for 7D-ligated group compared to sham-operated controls (28 ± 3.6 vs. 19.2 ± 5.1 for sham-operated group, $P < 0.001$). Following Fast Blue (FB) retrograde labeling, the total number of retrogradely labeled cells in the upper thoracic DRGs (T1–T3) was 25 ± 9 and in lower thoracic DRGs (T8–T10) were 48 ± 12. About one-third of FB-labeled cells were $P2X_3$ positive in sham-operated control rats (Fig. 7). However, no significant increase in the number of FB-labeled $P2X_3$ positive cells was observed in 7D-ligated animals. Similarly, in NGs, total number of retrogradely labeled

cells was 617 ± 32 ($n = 3$) with no significant difference in FB-labeled cells between two groups (Fig. 7).

Immunohistochemical analysis of $P2X_3$ coexpression pattern in DRGs and NGs

The distribution pattern of $P2X_3$ immunoreactivity in peptidergic and non-peptidergic small diameter C-fibers in DRGs and NGs are shown in Fig. 8a. We failed to observe a significant co-localization of $P2X_3$ and SP immunostaining in thoracic DRGs (4% of total $P2X_3$ positive cells). In contrast, majority (>85%) of these $P2X_3$-positive cells were also IB4 positive. In NGs, however, only 50% of $P2X_3$-positive cells were IB4-positive (Fig. 8a). Unlike $P2X_3$-positive cells in DRGs, a small percentage (20%) of $P2X_3$ positive cells in NGs also exhibited SP-immunoreactivity.

The co-localization of $P2X_3$ and TRPV1 immunoreactivities for DRGs and NGs is shown in Fig. 8b. Interestingly, a distinct population of small diameter TRPV1 positive cells failed to exhibit $P2X_3$ immunoreactivity. In DRGs from sham-operated animals, the intensity of TRPV1 immunostaining are significantly less compared to 7D-ligated group. Based on the cut off threshold selected for counting the cells with co-localization of TRPV1 and $P2X_3$, the number of $P2X_3$ positive cells with TRPV1 staining were significantly higher in both upper thoracic (T3) and lower thoracic (T8) DRGs from 7D-ligated animals compared to sham group ($P < 0.01$, Fig. 8c). Similarly, in NGs, the number of $P2X_3$ positive cells with TRPV1 staining was significantly higher for ligated animals compared to sham-operated controls ($P < 0.05$).

Discussion

Objective and summary data

Clinical observations suggest that acid exposure alters the sensory perception of the esophagus via sensitization of the primary sensory neurons leading to central sensitization (Hu et al. 2000; Mehta et al. 1995; Peghini et al. 1996; Sarkar et al. 2000). These clinical findings have been supported by recent experimental studies in cats documenting sensitization of spinal and brainstem neurons following noxious chemical stimulation of the esophagus (Garrison et al. 1992; Medda et al. 2005). Although these studies are acute in nature, it gives a clear indication that acid alters the functions of esophageal sensory neurons.

The objective of the present study was to investigate whether acid-reflux influence the expression of pro-nociceptive $P2X_3$ receptor in spinal and vagal sensory neurons. In this study, reflux was promoted by reducing the compliance and restricting gastric emptying surgically (Banerjee et al. 2007). Results indicate that reflux-induced esophagitis produces (1) significant increase in $P2X_3$ protein expression in thoracic DRGs and NGs, but not in the esophageal mucosa and muscle, (2) immunohistochemical analysis demonstrate increase in the intensity of $P2X_3$ expression in DRGs and NGs, (3) the intensity of $P2X_3$-TRPV1 co-expression is significantly higher in DRG and NG cells from 7D-ligated animals in comparison to sham-operated controls. However, unlike DRGs, 50% of $P2X_3$ positive cells in NGs fail to show IB4-binding and TRPV1-ir, indicating the presence of an additional

$P2X_3$-mediated downstream signaling mechanism of NG neurons. Most importantly, an upregulation of $P2X_3$ expression was observed both in upper and as well as in lower thoracic DRG neurons in reflux-induced esophagitis animals. This differential expression pattern of $P2X_3$ receptors in primary sensory neurons might contribute to altered esophageal sensitivity in esophagitis.

$P2X_3$ receptor and visceral nociception

$P2X_3$ receptor expression is predominantly in a subset of crest-derived sensory neurons, which represents a major component of ATP-gated ion channels in DRGs (Chen et al. 1995; Cook et al. 1997), whereas embryonic placode derived nodose neurons express both $P2X_3$ and $P2X_2$ subunits that are involved in ATP-mediated sustained inward current (Kwong et al. 2008). Recent studies also document purine-mediated sensitization of afferent neurons to various stimuli (Kress and Guenther 1999; Sawynok 1998). It is well recognized that this receptor plays an important role in signaling visceral pain. For example, distension of the colon triggers ATP release from the colorectal epithelium that activates sensory neurons via purinergic $P2X_3$ receptor (Wynn et al. 2003). Increase in expressions of $P2X_2$ and $P2X_3$ receptors and enhanced responses to purinergic agonist have also been documented in animal model of colonic inflammation (Wynn et al. 2004). Similarly, the excitatory effect of P2X purinoceptor agonist, α,β-methylene-ATP on vagal afferents following esophageal inflammation had been reported in ferrets (Page et al. 2000).

In the present study, the number of retrograde labeling from the distal esophagus, failed to show any difference following esophagitis. The total number of Fast Blue labeled cells in thoracic DRGs in the present study is higher than that reported earlier (Dütsch et al. 1998). This could be due to the use of different dye (Fluoro-Gold) and single administration contrast to four applications of Fast Blue in the present study. As for $P2X_3$-ir, in both DRGs and NGs, there was significant increase in the intensity in tissues from 7D-ligated animals compared to sham-operated controls. This finding was supported further by western blot analysis, where significant upregulation of $P2X_3$ protein expression was observed in both NGs and DRGs from 7D-ligated rats. In recent study in rats, about 40% of DRG neurons in the lumbar spinal cord (L4–L5) are reported to be $P2X_3$-positive (Vulchanova 1998), whereas, retrograde labeling from the mouse descending colon demonstrates 36% thoracolumber DRG neurons with $P2X_3$-ir compared to only 19% of lumbo-sacral neurons indicating a distinct difference in the receptor expression patterns at different level of spinal DRGs (Brierley et al. 2005).

Among different subtypes of P2X receptors, $P2X_2$ and $P2X_3$ receptors are expressed in small diameter sensory neurons in DRGs and thought to be involved in nociception (Bradbury et al. 1998; Dunn et al. 2001). In a recent study, 49% BDNF positive cells in NG is reported to be $P2X_3$ positive (Ichikawa et al. 2007), whereas in DRG neurons, approximately, 94% of the $P2X_3$ positive neuronal profiles are labeled by IB4 and 3% with SP-ir (Vulchanova et al. 1998). Moreover, single-cell RT–PCR analysis revealed that the NG neurons innervating the esophagus expressed mRNA for $P2X_2$ and $P2X_3$ subunits, whereas majority of DRG neurons innervating this tissue express only $P2X_3$ subunit (Kwong et al. 2008). The difference in the receptor expression pattern was also evident in the present

study, where the percentage of $P2X_3$-positive cells with IB4 and SP co-localization was markedly different between the DRGs and NGs, emphasizing, thereby, differences in their activation pathways, functional characters, and pharmacological properties.

Differential $P2X_3$ receptor expression between vagal and spinal pathways

Neonatal capsaicin treatment results in decrease in $P2X_3$-positive neurons by 70% and decrease sensitivity to noxious stimulation, which correlates well with the loss of IB4-binding neurons expressing $P2X_3$ receptors (Vulchanova et al. 1998). Studies in rodents and humans have documented that both $P2X_2$ and $P2X_3$ receptor expression is upregulated in cystitis and possibly contributing bladder hyperreflexia and pain (Dang et al. 2008; Nazif et al. 2007; Tempest et al. 2004). Exogenous application ATP and the P2X selective agonist α,β-methylene ATP sensitizes responses of afferents to distension and responses can be attenuated by non-selective P2X receptor blockers TNP-ATP and PPADS (Rong and Burnstock 2004; Rong et al. 2002; Wynn et al. 2003). In line with previous reports, our study documents that $P2X_3$ receptors upregulate after esophageal inflammation. We further investigated the co-expression of $P2X_3$ with TRPV1 in the spinal and vagal sensory neurons. Our results show that esophageal inflammation significantly increases the $P2X_3$ and TRPV1 immunostaining and co-expression of these two receptors in thoracic DRGs and NGs. This finding complements the previous reports of activation of homomeric $P2X_3$ receptors in peripheral terminals of capsaicin sensitive (i.e., TRPV1-positive) primary afferent fibers and their involvement in the induction of nocifensive behavior and thermal hyperalgesia (Burnstock 2006; Dunn et al. 2001).

Reflux-induced esophagitis also results in a significant increase in TRPV1 expression in DRGs and NGs (Banerjee et al. 2007). However, in the present study, only 40% of $P2X_3$ positive cells exhibit a significantly high immunostaining for TRPV1 in NG compared to 70% $P2X_3$-positive cells in DRGs with TRPV1 staining. This difference in $P2X_3$/TRPV1 co-expression between DRGs and NGs also emphasizes a difference in $P2X_3$ receptor-mediated signaling in spinal and vagal afferents.

Differential expression of $P2X_3$ mRNA and proteins in DRGs, NGs, and esophagus

In spite of significant upregulation of $P2X_3$ and TRPV1 receptor protein expressions in DRGs and NGs following esophagitis, we fail to detect any significant increase in mRNA expressions in upper thoracic DRGs and NGs. On the other hand, in esophageal muscle a significant upregulation of mRNA fail to demonstrate any increase in protein in the ligated animals. Our finding is very similar to recent observation in human patients with interstitial cystitis that exhibited a significant increase in $P2X_3$ protein expression accompanied with down regulation of $P2X_3$ gene expression in the urothelium (Tempest et al. 2004). This mismatch in mRNA and protein expression profiles could be due to complex relationship between mRNA and protein transcription and translation processes, which are governed by independent mechanisms and separate time constants (Lewandowski and Small 2005). There could also be a negative feedback between the level of protein and the rate of transcription of $P2X_3$ receptor gene.

$P2X_3$ expression pattern in neuronal and non-neuronal tissues

The difference in the molecular sizes of $P2X_3$ protein in DRGs, NGs, and esophageal tissues in this study emphasizes the heterogeneity in receptor expression among various tissues. In our study, $P2X_3$ protein expression in the esophageal tissue is at 64 kDa in contrast to 50 kDa in DRGs and NGs. Several other studies also indicate the differences in the molecular sizes of the receptor protein expression in various tissues. For example, in the rat urinary bladder, the $P2X_3$ expresses as a 75-kDa protein, but in human colon, the expression is at 66 kDa. In case of $P2X_3$ receptor, the intermediate bands (45–55 kDa) are observed in the culture, but not in the whole trigeminal ganglion (Simonetti et al. 2006; Studeny et al. 2005; Yiangou et al. 2000).

In human urothelium, $P2X_3$ receptor is reported to be expressed in a glycosylated form at a molecular weight of 64 kDa along with the deglycosylated form at 49 kDa, and in IC patients, an increase in glycosylated $P2X_3$ has also been reported (Tempest et al. 2004). In line with this finding, $P2X_3$ receptor in esophagus in the present study appears to be in glycosylated form, whereas in DRGs and NGs, the protein is predominantly in non-glycosylated form. Therefore, difference in sizes $P2X_3$ protein expressions in various tissues could be due to differences in glycosylation patterns of the receptors or possibly due to the existence of different isoforms and/or splice variants of mature receptor proteins in various tissues. The glycosylated and non-glycosylated proteins may also have different activation and functional pathways (Dunn et al. 2001; Jahnel et al. 2001).

Our finding is in contrast to previous studies reporting significant upregulation of $P2X_3$ receptor expression in nerve fibers and myenteric plexus of inflamed colons from patients with inflammatory bowel disease compared to normal individual (Yiangou et al. 2001). Similarly, there is a report of upregulation of $P2X_3$ receptors in urothelial cells from patients with interstitial cystitis (Sun and Chai 2004; Tempest et al. 2004). The difference in expression could depend on heterogeneity of tissues and different modes of stimuli.

In summary, our data indicate that reflux-induced esophagitis results in an increase in $P2X_3$ receptor expression and co-expression with TRPV1 in the thoracic DRGs and NGs with no significant difference in esophageal tissues. This result suggests a differential pattern of $P2X_3$ expression and co-expression in the DRGs and NGs may lead to different signaling mechanisms via spinal and vagal afferent pathways. Upregulation of $P2X_3$ receptors in sensory neurons following inflammation may contribute to altered sensation from the esophagus.

Acknowledgments

The study has been supported by NIH RO1 DK062312-01 awarded to Jyoti N. Sengupta and in part by NIH Grant 5R01 DK025731 awarded to Reza Shaker.

References

Banerjee B, Medda BK, Lazarova Z, Bansal N, Shaker R, Sengupta JN. Effect of reflux-induced inflammation on transient receptor potential vanilloid one (TRPV1) expression in primary sensory neurons innervating the oesophagus of rats. Neurogastroenterol Motil. 2007; 19:681–691. [PubMed: 17640184]

Bardoni R, Goldstein PA, Lee CJ, Gu JG, MacDermott AB. ATP P2X receptors mediate fast synaptic transmission in the dorsal horn of the rat spinal cord. J Neurosci. 1997; 17:5297–5304. [PubMed: 9204914]

Bradbury EJ, Burnstock G, McMahon SB. The expression of P2X3 purinoreceptors in sensory neurons: effects of axotomy and glial-derived neurotrophic factor. Mol Cell Neurosci. 1998; 12:256–268. [PubMed: 9828090]

Brierley SM, Carter R, Jones W III, Xu L, Robinson DR, Hicks GA, Gebhart GF, Blackshaw LA. Differential chemosensory function and receptor expression of splanchnic and pelvic colonic afferents in mice. J Physiol. 2005; 567:267–281. [PubMed: 15946967]

Burnstock G. Purinergic P2 receptors as targets for novel analgesics. Pharmacol Ther. 2006; 110:433–454. [PubMed: 16226312]

Chen CC, Akopian AN, Sivilotti L, Colquhoun D, Burnstock G, Wood JN. A P2X purinoceptor expressed by a subset of sensory neurons. Nature. 1995; 377:428–431. [PubMed: 7566119]

Cockayne DA, Hamilton SG, Zhu QM, Dunn PM, Zhong Y, Novakovic S, Malmberg AB, Cain G, Berson A, Kassotakis L, Hedley L, Lachnit WG, Burnstock G, McMahon SB, Ford AP. Urinary bladder hyporeflexia and reduced pain-related behaviour in P2X3-deficient mice. Nature. 2000; 407:1011–1015. [PubMed: 11069181]

Cook SP, Vulchanova L, Hargreaves KM, Elde R, McCleskey EW. Distinct ATP receptors on pain-sensing and stretch-sensing neurons. Nature. 1997; 387:505–508. [PubMed: 9168113]

Cooke HJ, Wunderlich J, Christofi FL. “The force be with you”: ATP in gut mechanosensory transduction. News Physiol Sci. 2003; 18:43–49. [PubMed: 12644618]

Dang K, Lamb K, Cohen M, Bielefeldt K, Gebhart GF. Cyclophosphamide-induced bladder inflammation sensitizes and enhances P2X receptor function in rat bladder sensory neurons. J Neurophysiol. 2008; 99:49–59. [PubMed: 17959738]

Dunn PM, Zhong Y, Burnstock G. P2X receptors in peripheral neurons. Prog Neurobiol. 2001; 65:107–134. [PubMed: 11403876]

Dütsch M, Eichhorn U, Wörl J, Wank M, Berthoud HR, Neuhuber WL. Vagal and spinal afferent innervation of the rat esophagus: a combined retrograde tracing and immuno cytochemical study with special emphasis on calcium-binding proteins. J Comp Neurol. 1998; 398(2):289–307. [PubMed: 9700572]

Evans RJ. The molecular biology of P2X receptors. J Auton Pharmacol. 1996; 16:309–310. [PubMed: 9131404]

Garrison DW, Chandler MJ, Foreman RD. Viscerosomatic convergence onto feline spinal neurons from esophagus, heart and somatic fields: effects of inflammation. Pain. 1992; 49:373–382. [PubMed: 1408304]

Guo A, Vulchanova L, Wang J, Li X, Elde R. Immunocytochemical localization of the vanilloid receptor 1 (VR1): relationship to neuropeptides, the P2X3 purinoceptor and IB4 binding sites. Eur J Neurosci. 1999; 11:946–958. [PubMed: 10103088]

Holzer P. Gastrointestinal afferents as targets of novel drugs for the treatment of functional bowel disorders and visceral pain. Eur J Pharmacol. 2001; 429:177–193. [PubMed: 11698040]

Hu WH, Martin CJ, Talley NJ. Intraesophageal acid perfusion sensitizes the esophagus to mechanical distension: a Barostat study. Am J Gastroenterol. 2000; 95:2189–2194. [PubMed: 11007216]

Ichikawa H, Terayama R, Yamaai T, Yan Z, Sugimoto T. Brain-derived neurotrophic factor-immunoreactive neurons in the rat vagal and glossopharyngeal sensory ganglia; co-expression with other neurochemical substances. Brain Res. 2007; 1155:93–99. [PubMed: 17512913]

Jahnel R, Dreger M, Gillen C, Bender O, Kurreck J, Hucho F. Biochemical characterization of the vanilloid receptor 1 expressed in a dorsal root ganglia derived cell line. Eur J Biochem. 2001; 268:5489–5496. [PubMed: 11683872]

Khakh BS, Humphrey PP, Surprenant A. Electrophysiological properties of P2X-purinoceptors in rat superior cervical, nodose and guinea-pig coeliac neurones. J Physiol. 1995; 484(Pt 2):385–395. [PubMed: 7602533]

Kirkup AJ, Brunsden AM, Grundy D. Receptors and transmission in the brain-gut axis: potential for novel therapies. I. Receptors on visceral afferents. I. Receptors on visceral afferents. Am J Physiol Gastrointest Liver Physiol. 2001; 280:G787–G794. [PubMed: 11292585]

Kress M, Guenther S. Role of [Ca2 +]i in the ATP-induced heat sensitization process of rat nociceptive neurons. J Neurophysiol. 1999; 81:2612–2619. [PubMed: 10368381]

Kwong K, Kollarik M, Nassenstein C, Ru F, Undem BJ. P2X2 receptors differentiate placodal vs. neural crest C-fiber phenotypes innervating guinea pig lungs and esophagus. Am J Physiol Lung Cell Mol Physiol. 2008; 295:L858–L865. [PubMed: 18689601]

Lewandowski NM, Small SA. Brain microarray: finding needles in molecular haystacks. J Neurosci. 2005; 25:10341–10346. [PubMed: 16280569]

Medda BK, Sengupta JN, Lang IM, Shaker R. Response properties of the brainstem neurons of the cat following intra-esophageal acid-pepsin infusion. Neuroscience. 2005; 135:1285–1294. [PubMed: 16165290]

Mehta AJ, De Caestecker JS, Camm AJ, Northfield TC. Sensitization to painful distention and abnormal sensory perception in the esophagus. Gastroenterology. 1995; 108:311–319. [PubMed: 7835571]

Nazif O, Teichman JM, Gebhart GF. Neural upregulation in interstitial cystitis. Urology. 2007; 69:24–33. [PubMed: 17462476]

Novakovic SD, Kassotakis LC, Oglesby IB, Smith JA, Eglen RM, Ford AP, Hunter JC. Immunocytochemical localization of P2X3 purinoceptors in sensory neurons in naive rats and following neuropathic injury. Pain. 1999; 80:273–282. [PubMed: 10204740]

Omura N, Kashiwagi H, Chen G, Suzuki Y, Yano F, Aoki T. Establishment of surgically induced chronic acid reflux esophagitis in rats. Scand J Gastroenterol. 1999; 34:948–953. [PubMed: 10563662]

Page AJ, O'Donnell TA, Blackshaw LA. P2X purinoceptor-induced sensitization of ferret vagal mechanoreceptors in oesophageal inflammation. J Physiol. 2000; 523(Pt 2):403–411. [PubMed: 10699084]

Peghini PL, Johnston BT, Leite LP, Castell DO. Mucosal acid exposure sensitizes a subset of normal subjects to intra-oesophageal balloon distension. Eur J Gastroenterol Hepatol. 1996; 8:979–983. [PubMed: 8930562]

Robinson DR, McNaughton PA, Evans ML, Hicks GA. Characterization of the primary spinal afferent innervation of the mouse colon using retrograde labelling. Neurogastroenterol Motil. 2004; 16:113–124. [PubMed: 14764211]

Rong W, Burnstock G. Activation of ureter nociceptors by exogenous and endogenous ATP in guinea pig. Neuropharmacology. 2004; 47:1093–1101. [PubMed: 15555643]

Rong W, Spyer KM, Burnstock G. Activation and sensitisation of low and high threshold afferent fibres mediated by P2X receptors in the mouse urinary bladder. J Physiol. 2002; 541:591–600. [PubMed: 12042363]

Sarkar S, Aziz Q, Woolf CJ, Hobson AR, Thompson DG. Contribution of central sensitisation to the development of non-cardiac chest pain. Lancet. 2000; 356:1154–1159. [PubMed: 11030295]

Sawynok J. Adenosine receptor activation and nociception. Eur J Pharmacol. 1998; 347:1–11. [PubMed: 9650842]

Sawynok J, Reid A. Peripheral adenosine 5′-triphosphate enhances nociception in the formalin test via activation of a purinergic p2X receptor. Eur J Pharmacol. 1997; 330:115–121. [PubMed: 9253943]

Simonetti M, Fabbro A, D'Arco M, Zweyer M, Nistri A, Giniatullin R, Fabbretti E. Comparison of P2X and TRPV1 receptors in ganglia or primary culture of trigeminal neurons and their modulation by NGF or serotonin. Mol Pain. 2006; 2:11. [PubMed: 16566843]

Studeny S, Torabi A, Vizzard MA. P2X2 and P2X3 receptor expression in postnatal and adult rat urinary bladder and lumbosacral spinal cord. Am J Physiol Regul Integr Comp Physiol. 2005; 289:R1155–R1168. [PubMed: 15947072]

Sun Y, Chai TC. Up-regulation of P2X3 receptor during stretch of bladder urothelial cells from patients with interstitial cystitis. J Urol. 2004; 171:448–452. [PubMed: 14665953]

Tempest HV, Dixon AK, Turner WH, Elneil S, Sellers LA, Ferguson DR. P2X and P2X receptor expression in human bladder urothelium and changes in interstitial cystitis. BJU Int. 2004; 93:1344–1348. [PubMed: 15180635]

Vulchanova L, Riedl MS, Shuster SJ, Buell G, Surprenant A, North RA, Elde R. Immunohistochemical study of the P2X2 and P2X3 receptor subunits in rat and monkey sensory neurons and their central terminals. Neuropharmacology. 1997; 36:1229–1242. [PubMed: 9364478]

Vulchanova L, Riedl MS, Shuster SJ, Stone LS, Hargreaves KM, Buell G, Surprenant A, North RA, Elde R. P2X3 is expressed by DRG neurons that terminate in inner lamina II. Eur J Neurosci. 1998; 10:3470–3478. [PubMed: 9824460]

Wynn G, Rong W, Xiang Z, Burnstock G. Purinergic mechanisms contribute to mechanosensory transduction in the rat colorectum. Gastroenterology. 2003; 125:1398–1409. [PubMed: 14598256]

Wynn G, Ma B, Ruan HZ, Burnstock G. Purinergic component of mechanosensory transduction is increased in a rat model of colitis. Am J Physiol Gastrointest Liver Physiol. 2004; 287:G647–G657. [PubMed: 15331354]

Xiang Z, Burnstock G. Development of nerves expressing P2X3 receptors in the myenteric plexus of rat stomach. Histochem Cell Biol. 2004; 122:111–119. [PubMed: 15258768]

Xiang Z, Bo X, Burnstock G. Localization of ATP-gated P2X receptor immunoreactivity in rat sensory and sympathetic ganglia. Neurosci Lett. 1998; 256:105–108. [PubMed: 9853714]

Yiangou Y, Facer P, Birch R, Sangameswaran L, Eglen R, Anand P. P2X3 receptor in injured human sensory neurons. Neuroreport. 2000; 11:993–996. [PubMed: 10790870]

Yiangou Y, Facer P, Baecker PA, Ford AP, Knowles CH, Chan CL, Williams NS, Anand P. ATP-gated ion channel P2X(3) is increased in human inflammatory bowel disease. Neurogastroenterol Motil. 2001; 13:365–369. [PubMed: 11576396]

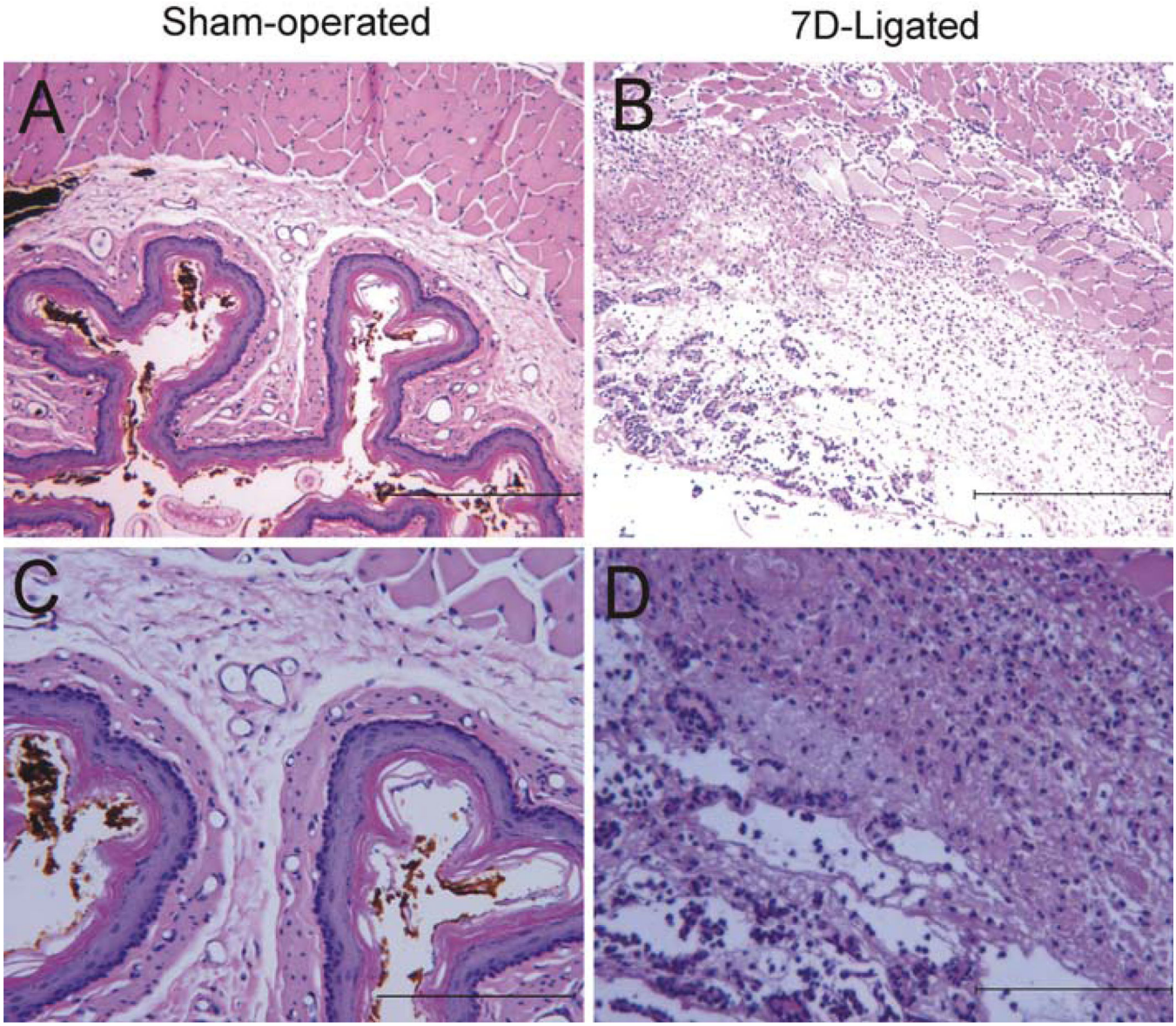

Fig. 1.

H&E stained transversed sections of distal esophagus from 7D-ligated and sham-operated rats. **a** Sham-operated esophagus exhibited intact mucosal layer and no inflammatory cell infiltration. **b** 7D-ligated esophagus demonstrated edema of epithelial cell layers, submucosal hyperplasia and inflammatory cell infiltrates. **c** Esophageal section from sham-operated rat at higher magnification. d Esophageal section from 7D-ligated rat at higher magnification. The *scale bars* for **a** and **b** are 200 μm and **c** and **d** are 100 μm

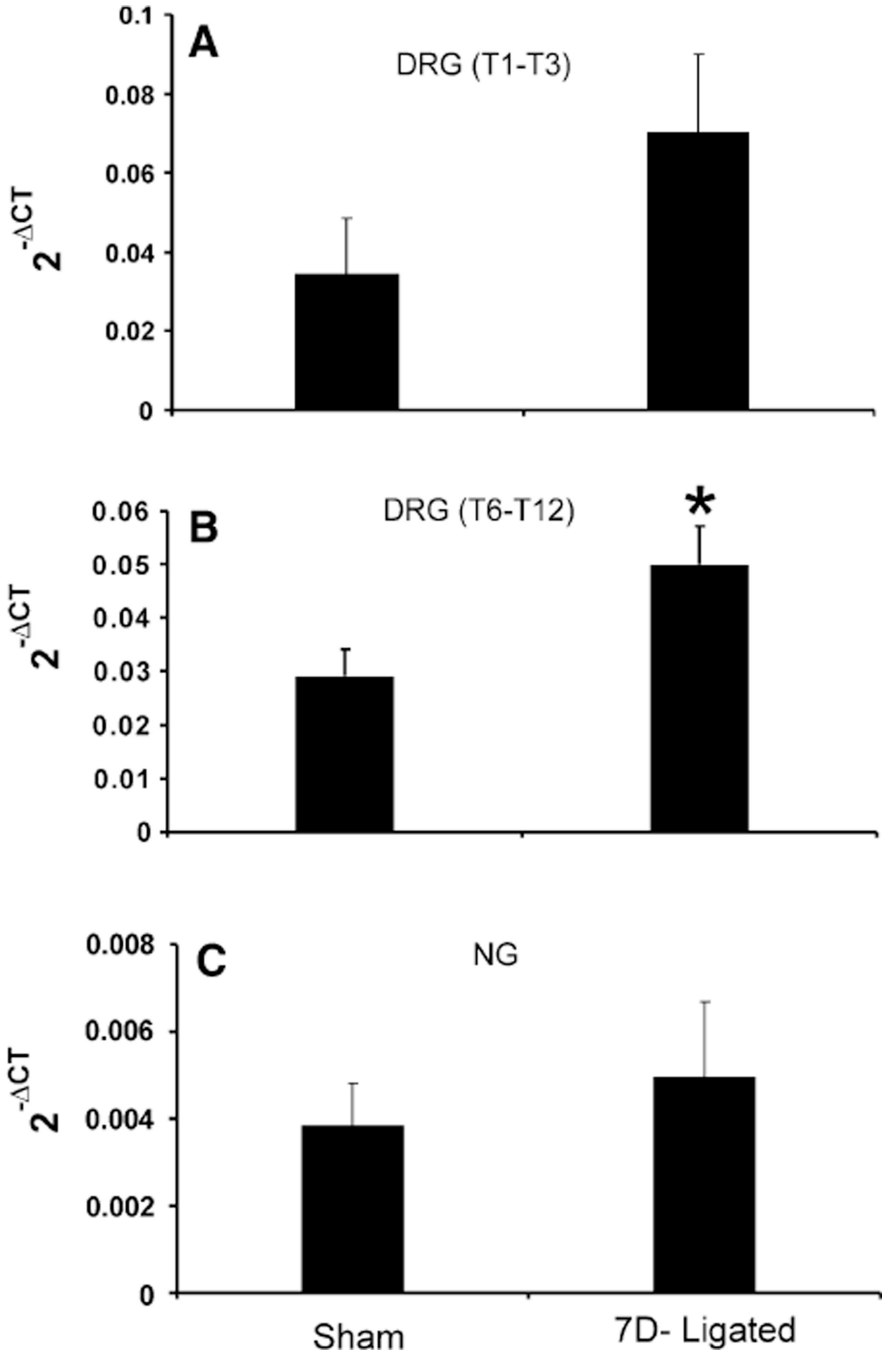

Fig. 2.

Real time RT–PCR for $P2X_3$ gene expression in the thoracic DRGs and NGs from 7D-ligated and sham-operated rats. **a** In DRGs, cDNAs from respective groups were amplified using primers for $P2X_3$. **b** In NGs, cDNAs from respective groups were amplified using primers for $P2X_3$. ΔC_T indicates the difference between the number of cycles necessary to detect the PCR products of the experimental gene and the reference gene. Ordinate values $(2^{\Delta C}_{T})$ correspond to the receptor mRNA expression relative to the reference gene in the tissue. Values are the mean ± SD of three real time PCR determinations

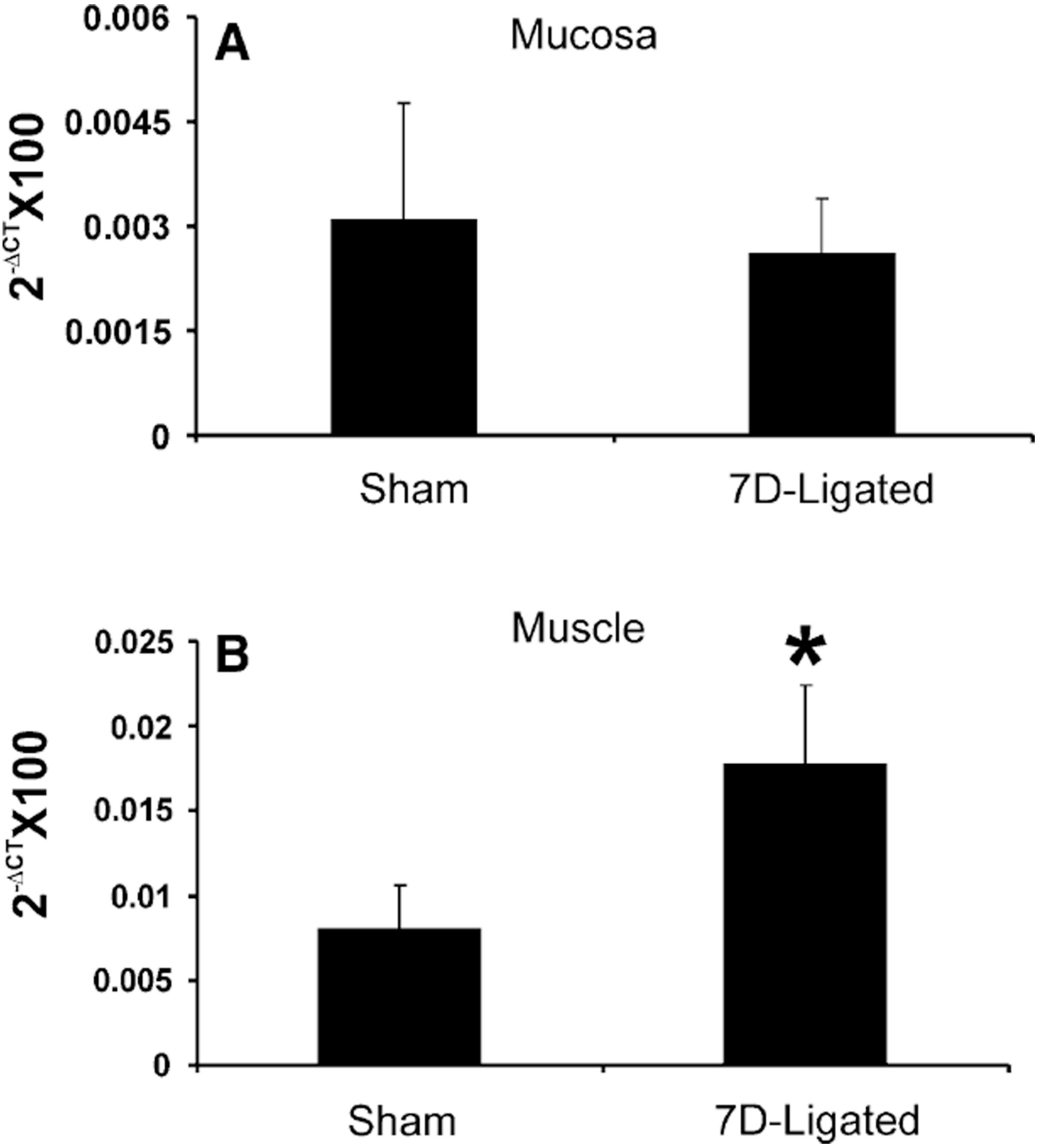

Fig. 3.

Real time RT–PCR for $P2X_3$ gene expression in the esophageal mucosa and muscle preparations from 7D-ligated and sham-operated rats. **a** In mucosa, cDNAs from respective groups were amplified using primers for $P2X_3$. **b** In muscle, cDNAs from respective groups were amplified using primers for $P2X_3$. ΔC_T indicates the difference between the number of cycles necessary to detect the PCR products of the experimental gene and the reference gene GAPDH. Ordinate values $(2^{\Delta C}_{T})$ correspond to the receptor mRNA expression relative to the

reference gene in the tissue. Values are the mean ± SD of three real time PCR determinations (*$P < 0.05$)

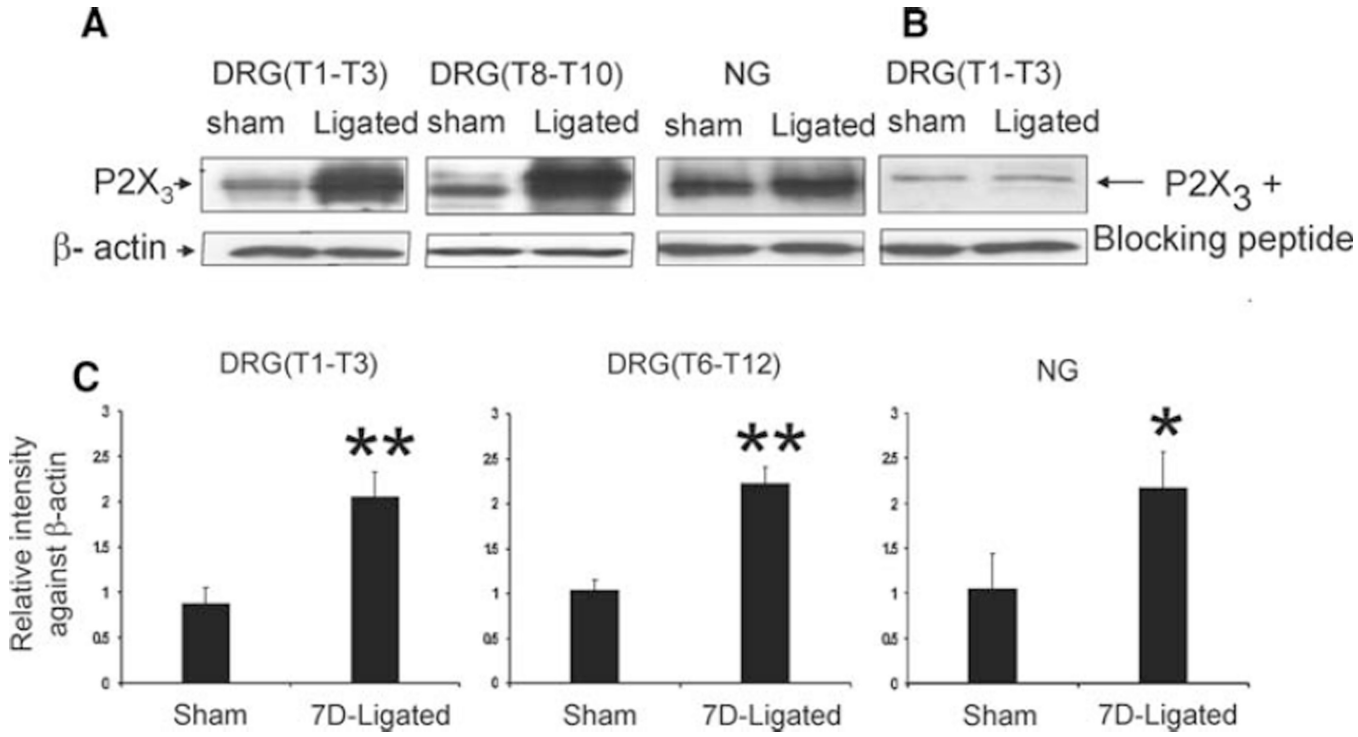

Fig. 4.

Western blot analysis of thoracic DRGs and NGs for $P2X_3$ receptor protein expression in reflux esophagitis (7D-ligated) and sham-operated rats. β-actin staining was used as a reference protein. **a** $P2X_3$ protein was expressed in the molecular weight range of 55–50 kDa. **b** preabsorption of $P2X_3$ antibody with immunogen (10 μM) eliminated the band at 50 kDa. **c** histogram of relative $P2X_3$ band density in the experimental and control groups were normalized to β-actin staining. $P2X_3$ receptor expression in the DRGs and NGs demonstrated a significant upregulation in 7D-ligated group compared with expression in sham-operated controls. The results were expressed as mean ± SD of three experiments (** $P < 0.01$, * $P < 0.05$)

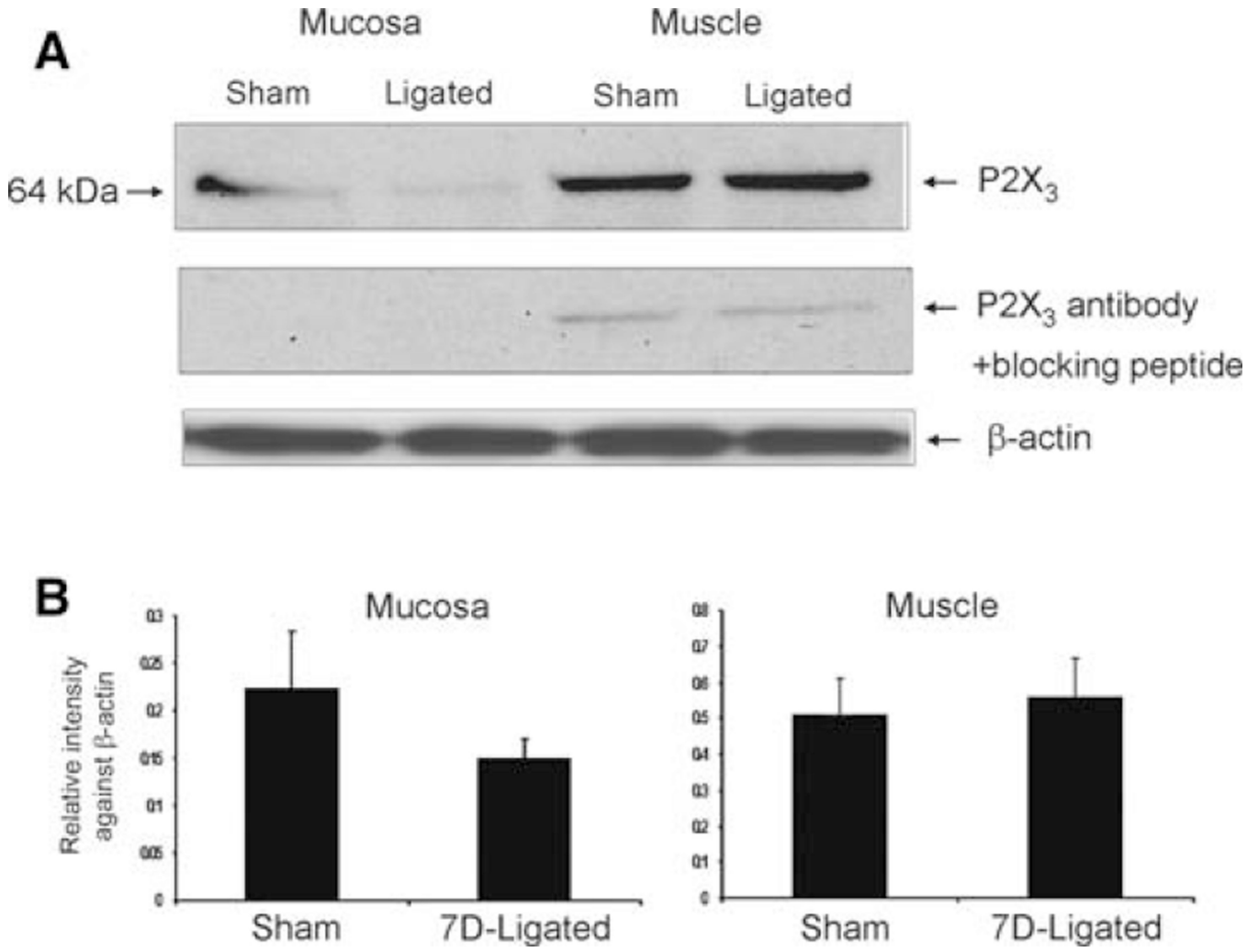

Fig. 5.

Western blot analysis of esophageal mucosa and muscle for $P2X_3$ receptor protein expression in reflux esophagitis (7D-ligated) and sham-operated rats. β-actin immunostaining was used as a reference protein. **a** $P2X_3$ was expressed as a 64 kDa protein both in esophageal mucosa and muscle extracts. Preabsorption of $P2X_3$ antibody with immunogen (10 μM) completely eliminated the immunoreactivity in the mucosa and 90% in the muscle preparation. **b** Histograms of relative $P2X_3$ band density in the experimental and control groups were normalized to β-actin staining. The results were expressed as mean ± SD of three experiments

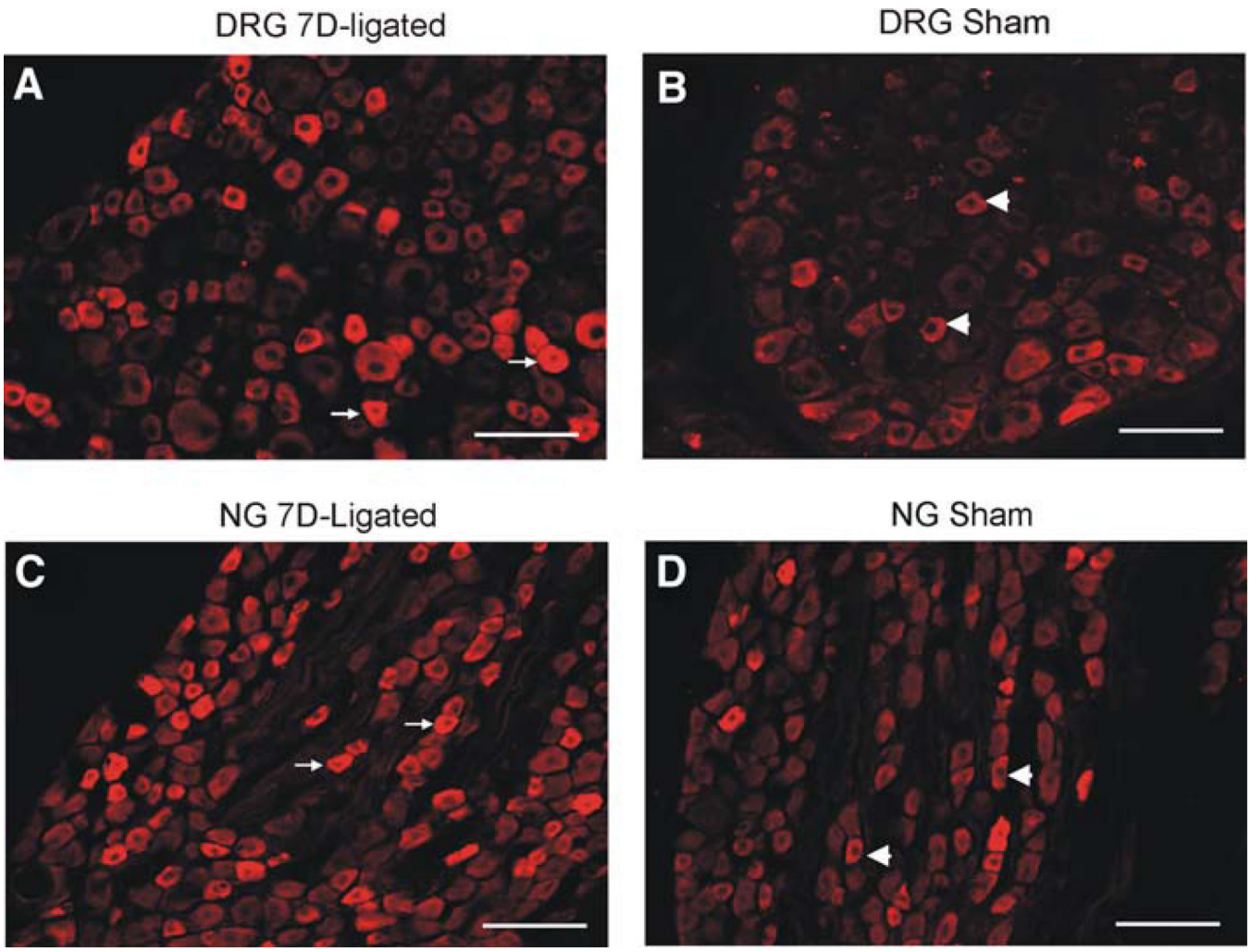

Fig. 6.

Photomicrography of $P2X_3$ immunoreactivities in the thoracic DRGs (T3) and NGs. **a** Immunostaining of DRG section from 7D-ligated rats. **b** Immunostaining of DRG (T3) section from sham-operated controls. **c** Immunostaining of NG section from 7D-ligated rats. **d** Immunostaining of NG section from sham-operated controls. *Arrows* indicate high intensity of $P2X_3$ labeling and arrow heads identify the cells with low intensity small diameter cells. The *scale bar* is 100 μm

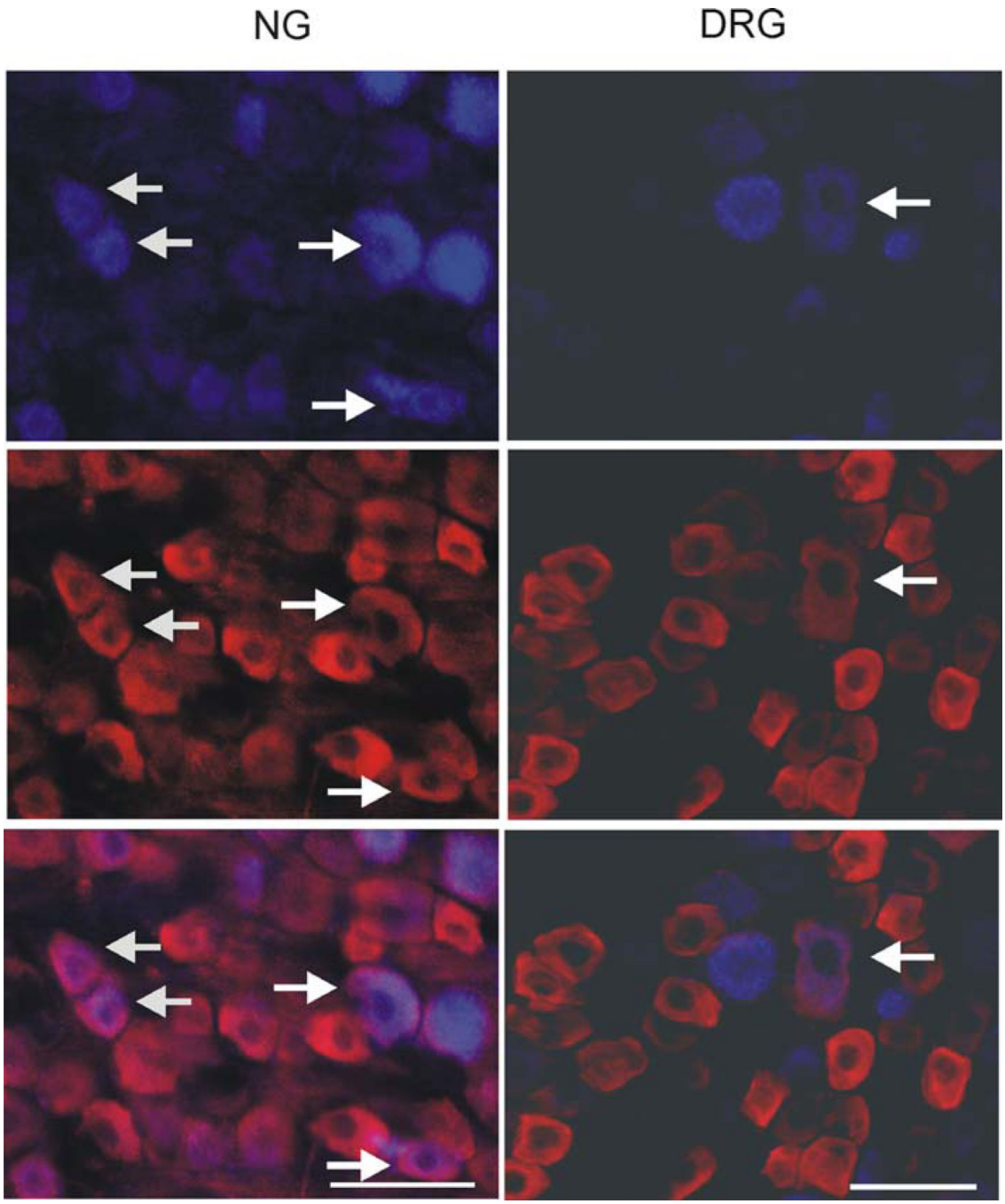

Fig. 7.

Photomicrography of P2X3 immunoreactivity in the NG and thoracic (T8) DRG retrogradely labeled with Fast Blue (FB). FB was injected in the subdiaphragmatic segment of the esophagus and FB positive cell bodies in the NG (*left column*) and DRG (*right column*) were examined for immunoreactivity with P2X3 antibody. *Arrows* indicate cells in NG and DRG with FB and P2X3 co-localization. The *scale bar* is 50 μm

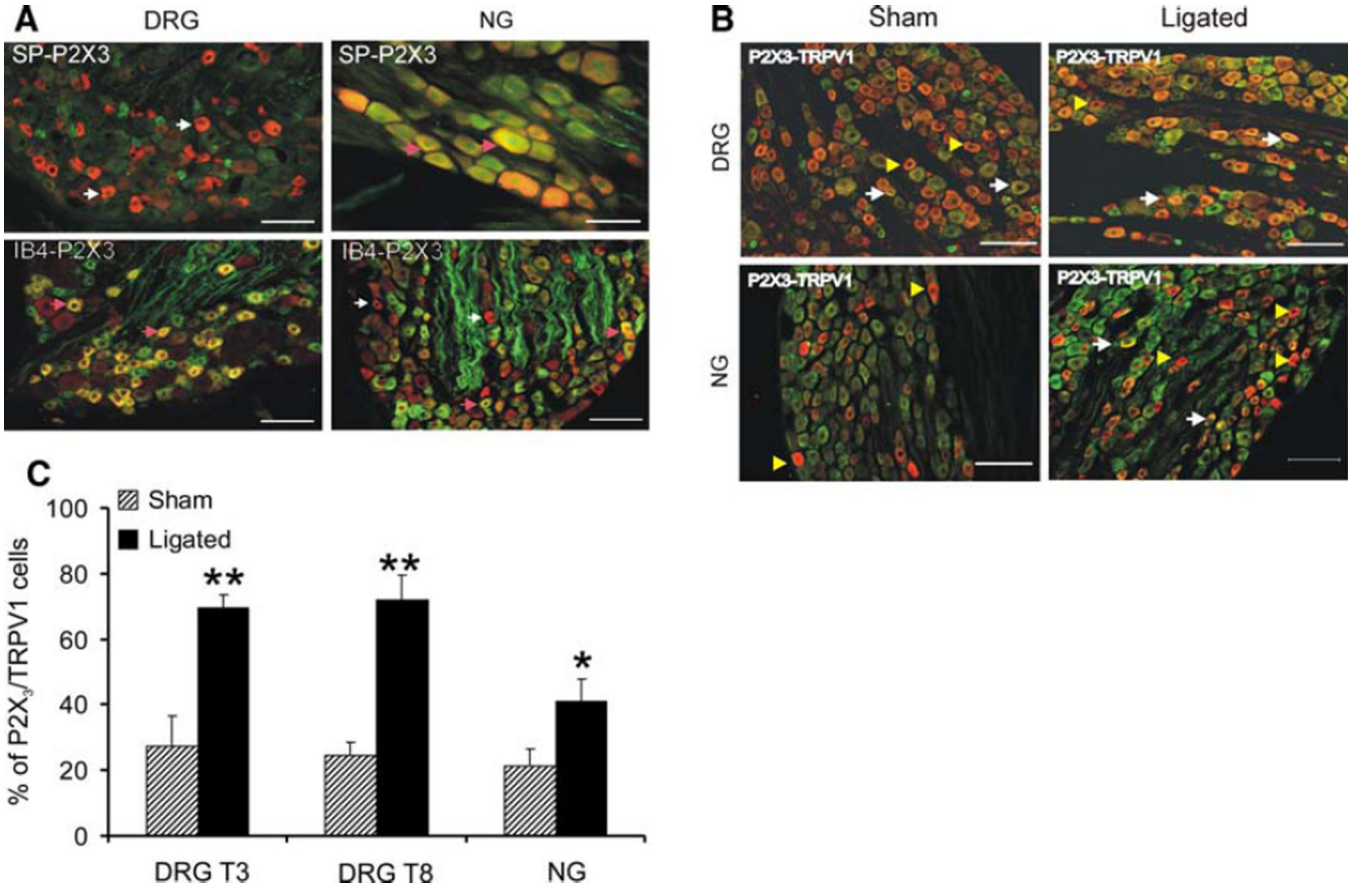

Fig. 8.

a Distribution pattern of $P2X_3$ immunoreactivity in peptidergic and non peptidergic small diameter c-fibers in DRG (T3) and NG. DRG sections from sham-operated rat with P2X3-SP immunostaining (*left column, upper panel*) and P2X3-IB4 staining (*left column, lower panel*). NG sections from sham-operated rat with P2x3-SP staining (*right column, upper panel*) and P2X3-IB4 staining (*right column, lower panel*). In the DRGs 85% of $P2X_3$ immunopositive cells was IB4-positive in comparison to 50% in the NGs. For P2X3-SP immunostaining 4% in DRGs and 20% NGs showed coexpression. *Arrows* (*pink*) indicate P2X3 positive cells with IB4 or SP immunostaining and *arrows* (*white*) indicate $P2X_3$-positive cells without IB4 or SP binding. The *scale bar* is 100 μm. **b** Coexpression of $P2X_3$-positive cells with TRPV1 in DRGs and NGs. A representative double immunostaining in the DRGs (T8) is as follows: sham-operated (*left column, upper panel*) and 7D-ligated rats (*right column, upper panel*). For NGs, sham-operated (*left column, lower panel*) and for 7D-ligated (*right column, lower panel*). Both in DRGs and NGs coexpression of TRPV1 in $P2X_3$-positive cells were significantly higher in 7D-ligated animals compared to sham-operated controls ($*P < 0.05$). *Arrows* indicate P2X3-positive cells coexpressing TRPV1 and *arrow heads* indicate P2X3-positive cells without TRPV1 immunostaining. The *scale bar* is 100 μm. **c** Analytical data of P2X3 and TRPV1 co expression in thoracic DRGs and NGs from 7D-ligated and sham-operate rats. The percentage of P2X3-and TRPV1 double

labeling is significantly high in thoracic DRGs T3 and T8 and in NGs (**$P < 0.01$, *$P < 0.05$ vs. sham-operated controls)